Flame speed measurements in turbulent dispersions of liquid fuels

Pedro M. de Oliveira, Tomoki Higuchi*, Patton M. Allison, Epaminondas Mastorakos

Hopkinson Laboratory, Department of Engineering,
University of Cambridge, Cambridge, UK.

*Koichi Hishida Laboratory, Department of Integrated Design Engineering,
Keio University, Kanagawa, Japan.

1 Introduction

The issue of flame speed in spray flows has been reviewed previously [1, 2], showing that the presence of the droplets in the flow as the flame propagates is usually detrimental to the flame speed [3]. This effect is attributed to the additional energy needed to fully evaporate the fuel droplets. Some numerical [4, 5] and experimental [6] works have shown, however, that the flame speed in specific conditions of small droplet size, degree of fuel prevaporization, and turbulence, can be larger than the equivalent flame speed in gaseous systems. Additional phenomena such as droplets surviving the flame front, flame propagation through preferential paths in the gaseous phase, or droplets of multi-component fuels, add to increasing complexity in such systems. Especially for the case of turbulent flow, where the turbulence is expected to increase the flame surface area and hence lead to fast turbulent flame speed – but at the same time may strain droplet-scale reaction zones or promote evaporation – there is no clear consensus on the effect of turbulence on the flame speed in sprays [6–9]. Thus more canonical experiments are needed in order to understand the underlying physics of such processes.

The objective of this work is to measure the flame speed of multi-component fuel dispersions in a turbulent air flow, where the mean and turbulent velocities and the droplet number density and size are homogeneous in space. Ignition is provided at a point and the spherically-expanding flame is observed, allowing for measurements of turbulent flame speed in sprays.

2 Experimental work

The experimental apparatus used in this work is the same as described by [10], and shown in Fig. 1. For the sake of completeness, it is briefly described here. The setup consists of two air lines and a fuel line connected to a divergent-convergent tube [11], i.e. the burner (1). Inside the burner, an air-assisted atomizer (2) injects the liquid into a preheated air stream. The air is prepared using a particulate and a coalescent

Correspondence to: pm580@cam.ac.uk

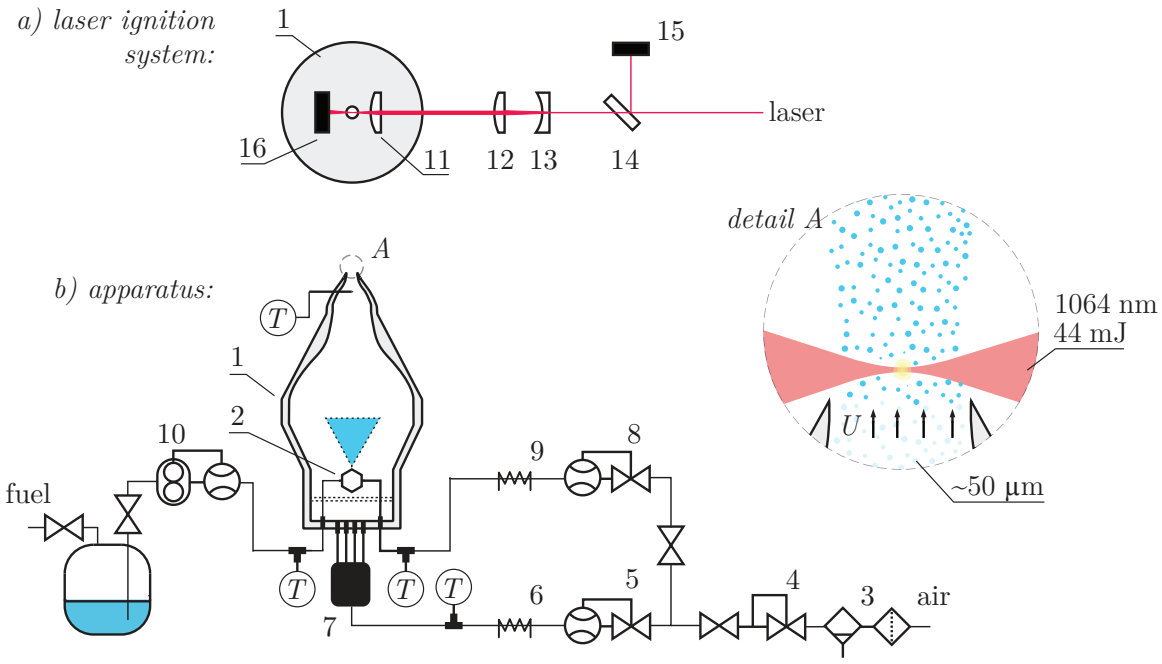

Figure 1: Schematic representation of the (a) the laser ignition system and (b) the apparatus [10].

filter (3) and a pressure regulator (4), and the flows are set with two flow controllers (5,8) and two PID-controlled in-line heaters (6,9). Additionally, a flow splitter (7) is used to evenly distribute the air flow at the bottom of the burner. The fuel is pumped at room temperature using a Coriolis mass flow meter and a gear pump (10). As the air flow carries the fuel droplets through a 20.8-mm diameter nozzle, a two-phase jet is formed, consisting of a mixture of liquid droplets, vapour, and air. Attention is given to the region of one nozzle diameter, where the flow is still uniform and the shear layers with the ambient air have not grown enough to affect the measurement region; therefore, the interrogation area is treated as uniform in all statistical measures, being convected uniformly downstream by the bulk velocity.

Three fuels were used: Jet A (codes as A2), and two alternative fuels being studied under the United States' National Jet Fuel Combustion Program (NJFCP) – an alcohol-to-jet fuel (C1), and a flat-boiling fuel (C5) [12]. C5 presents the highest volatility of the three fuels, while C1 is slightly less volatile and exhibits a distillation curve over a broader temperature span, and A2 is significantly less volatile than the others.

Ignition is performed by focusing the beam of a Nd-YAG laser (10 Hz, 1064 nm, 44 mJ) at the center of the jet and approximately 5 mm downstream of the nozzle. For that, a 30-mm plano-convex lens (11) is used, plus a 75-mm plano-convex (12) lens and a -30-mm plano-concave lens (13), allowing for a very small spark region. The energy at each attempt is before and after the flow with a beam splitter (14) energy sensors (15,16).

Experiments were carried out for the three above-mentioned fuels (A2, C5, and C1) with varying air bulk velocity ($U = 6$–15 m/s), and varying equivalence ratio ($\phi = 0.9$–2.1). The carrier air preheat temperature was set from 50 to 100 °C, resulting in some prevaporization of the fuel.[1]. The growth of the flame kernels

[1]The Sauter Mean Diameter in an *ethanol* spray in the same burner [11] was measured as $\sim$50 μm for similar flow conditions.

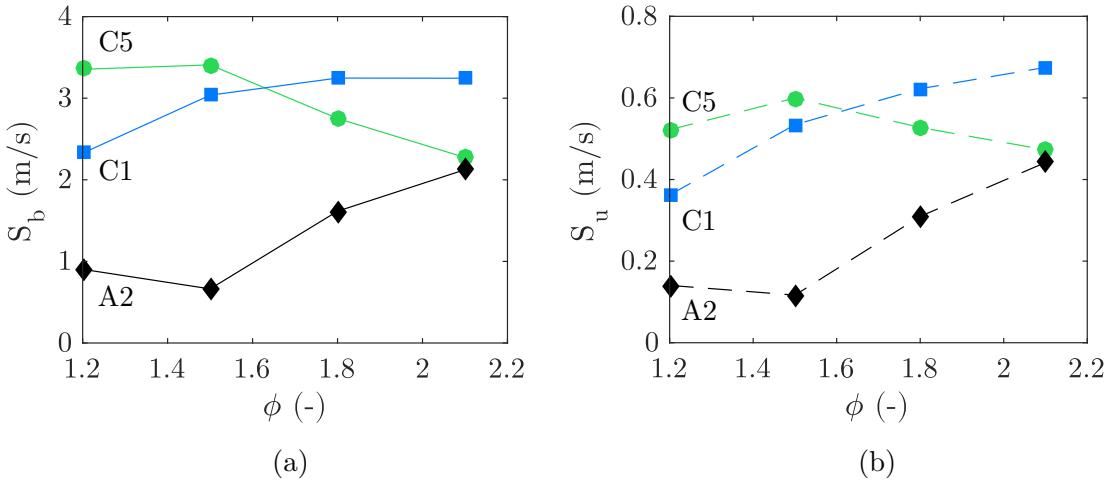

Figure 2: Measured (a) burned and (b) unburned flame speeds for A2, C5, and C1 in terms of the equivalence ratio – U =6 m/s, T =70 °C.

and its development into a self-sustaining flame was evaluated by high-speed Schlieren as well as OH*-chemiluminescence visualization for 2.6 ms after the spark, at 12 kHz, in a 20x20 mm window. For each test condition, 450 ignition attempts were performed.

The flame speed of the burned gases S_b was measured from the OH*-chemiluminescence data assuming a spherically propagating flame. By evaluating the maximum width and height of the flame at each visualization frame, the speed of the flame in the horizontal direction, that is, the speed the flame moves relative to the centroid of the kernel, was calculated as being $S_b(t) = \Delta w_t/2\Delta t$, where Δw_t is the change in width from frame to frame with a Δt time interval. The burned flame speed was also evaluated in the vertical direction. From these calculations, an average value between the horizontal and vertical burned flame speeds was obtained taking into account only successful ignition events (defined by an increasing OH* signal over time [10]). Finally, for each flow condition and successful ignition events, S_b was averaged in respect to time within a time window where plasma effects were no longer observed.

The unburned flame speed S_u was evaluated as being, $S_u = S_b\rho_b/\rho_u$ where ρ_b and ρ_u are the density of the burned and unburned gases respectively. Here, a series of approximations were made to estimate ρ_b and ρ_u, since the local equivalence ratio at which the flame burns is unknown, and there is the possibility of liquid droplets surviving the flame and being found in the burned zone. In this first approach, the unburned and burned densities were calculated based on the density of air at the measured reactants temperature at the nozzle, and at the adiabatic flame temperature evaluated for the given mixture based on the overall equivalence ratio (numerical data were taken from [12]).

3 Results

The results of the time-averaged burned flame speed and the unburned flame speed were plotted in terms of the equivalence ratio, and are shown in Figure 2. In both figures (a,b), the effect of the fuel volatility can be clearly observed: C5 is the most volatile fuel, and presents the highest flame speed at $\phi = 1.2$, followed by C1, and finally A2 that is the fuel that presents the lowest saturation pressure. The differences

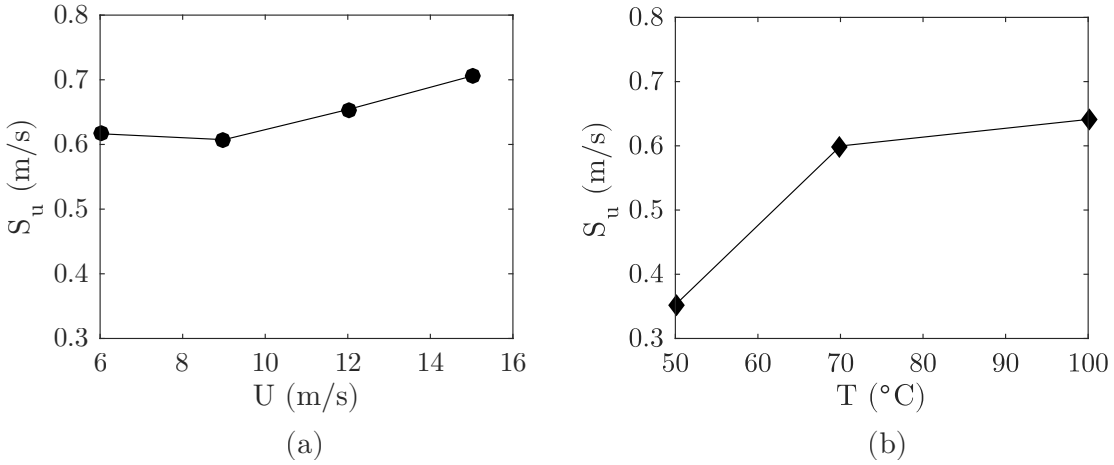

Figure 3: Unburned flame speed for C5 at $\phi = 1.5$, with varying (a) flow bulk velocity ($T = 70\,^{\circ}$C) and (b) temperature ($U = 6$ m/s).

between the fuels decrease as the mixture becomes richer. This results can also be interpreted in terms of the gaseous equivalence ratio ϕ_g, that is, the "effective equivalence ratio" seen by the flame propagating in the gas phase [13]. In the case of C5, as ϕ increases ϕ_g may have reached stoichiometry at about $\phi = 1.5$ – then, further increase of the overall equivalence ratio ϕ resulted in a rich gaseous phase and, therefore, a decrease in flame speed. Additionally, both C1 and A2 should be below stoichiometry in the gas phase, since there is an overall increase of the flame speed as ϕ increases. Also, the lower volatility of A2 results in a much lower flame speed than C1.

Figure 3 shows the unburned flame speed for C5 for varying (a) flow bulk velocity and (b) preheat temperature. The effect of the bulk velocity and temperature was seen to increase S_u for the present experimental conditions as both parameters increase. The values shown in Fig. 3 are slightly higher than the laminar burning velocity of the gaseous stoichiometric flame for a similar temperature ($\sim$0.6 m/s). Thus, it suggests that the accelerating effect due to turbulence[2] overcame the detrimental effect due to the presence of the droplets and the fact that the residence time of the droplets decreases as U increases, resulting in a lower amount of prevaporized fuel. As temperature increases for a constant U (Fig. 3b), the degree of prevaporization of the fuel increases. Thus, a larger flame speed was observed as ϕ_g likely approached stoichiometry. In order to further explore these results, measurements of turbulence and prevaporization are needed.

The visualization of a single ignition event in C1 was performed using Schlieren and OH* (Fig 4a). The Schlieren camera was positioned opposite and tilted in relation to the OH* camera, and resulting images were flipped in the vertical axis for convenience. Both image sequences (with Δt=250 μs) show the growing toroidal kernel created by the spark just before the first frame at the bottom (laser beam from right to left). Observing the Schlieren sequence, one should note that the focused beam gave rise to a number of ignition sites in the vicinity of focus point, mainly on the right side of the figure (i.e., closer to the source). However, two main points should be noted. First, these smaller kernels did not grow nor merge with the main kernel produced in the focus point. Second, these small kernels were not observed in the OH* visualization, thus

[2]Due to the shear produced at the meshes upstream of the atomizer and at the spray, the turbulent intensity at the exit of the burner is approximately u'/U= 10% [11].

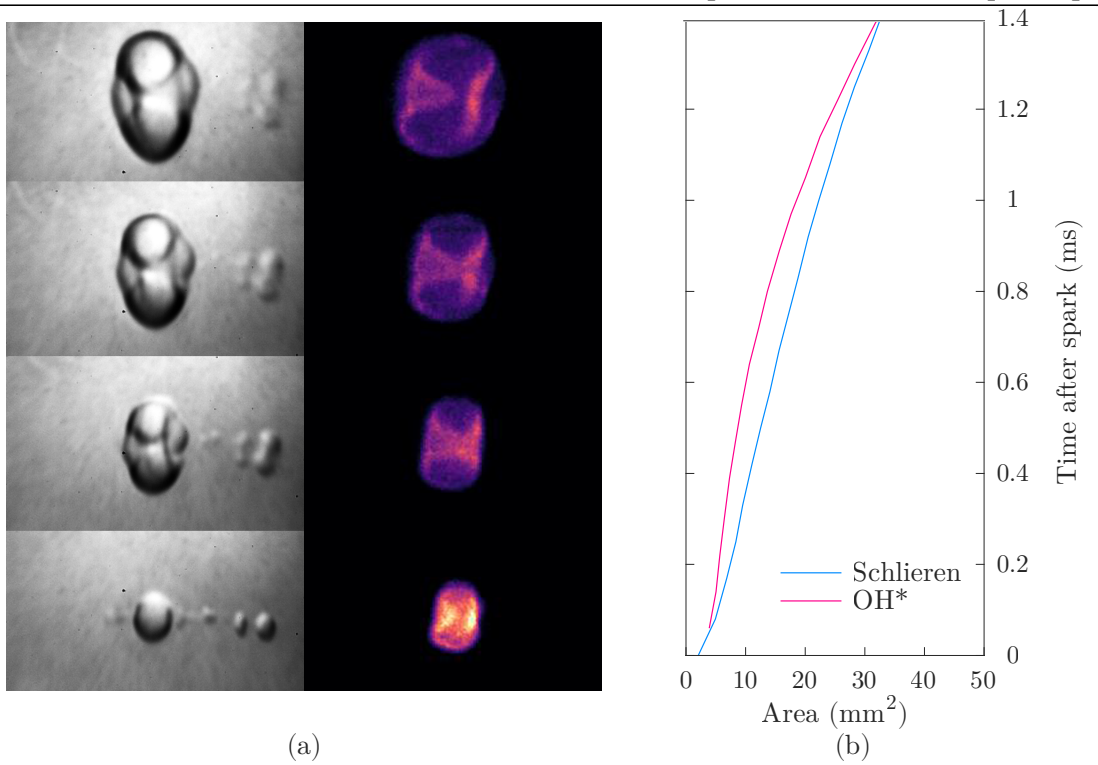

Figure 4: (a) Visualization of the ignition event using Schlieren (left) and OH*-chemiluminesce (right). (b) Area calculated based on OH* and Schlieren. Figures show results for C1, $\phi = 1.5$, U =6 m/s, T =70 °C.

indicating that although the Schlieren shows a significant decrease in density of that region, the temperature was not high enough in order to initiate the vigorous burning of the flame. Other comparisons between the OH* and Schlieren visualizations were performed, as in Fig. 4b, that shows the area of the kernel calculated based on both visualization techniques and plotted in terms of the time after the spark. Small differences in the area calculated by both methods were noticed. A supplementary video of OH* visualizations of different fuels and flow conditions is available online[3].

4 Conclusion

The present work experimentally evaluated the flame speed in three multi-component fuels – a conventional Jet A, a (alternative) comercial alcohol-to-jet fuel, and a flat-boiling curve surrogate fuel – by looking at the problem of a spherically expanding flame in a uniform turbulent droplet dispersion. The burned flame speed was measured, and the unburned flame speed was estimated based on these measurements and additional data for each fuel. Overall, the experiments have shown that the flame speed was lower in A2 (Jet A), probably due to its lower volatility, and increased with an increasing equivalence ratio. However, the same was not observed for C5 due to its higher volatility; for this fuel, the flame speed decreased with an overall increase of the equivalence ratio, likely due to rich conditions of the gaseous mixture. In order to precisely evaluate the flame speed and the effects of the spray and turbulence in such flows, a more detailed characterization of the flow in terms of droplet size, velocity, and degree of prevaporization is needed.

[3] https://vimeo.com/pedromo/laser-ignition-liquid-dispersions

Acknowledgments

PMO would like to thank the financial support of the Brazilian Space Agency and Brazil's National Council for Scientific and Technological Development. TH is grateful for the support of GESL Program of Keio University funded by Japan's Ministry of Education, Culture, Sports, Science and Technology. The authors also thank Dr. Tim Edwards at the US Air Force Research Lab for providing the fuels under the auspices of the NJFCP, Dr. Med Colket, and acknowledge the funding from the EU Clean Sky project AMEL.

References

[1] S. Aggarwal, "A review of spray ignition phenomena: Present status and future research," *Progress in Energy and Combustion Science*, vol. 24, no. 95, pp. 565–600, 1998.

[2] E. Mastorakos, "Forced ignition of turbulent spray flames," *Proc. of the Combustion Institute*, pp. 1–39, oct 2016.

[3] D. R. Ballal and A. H. Lefebvre, "Flame propagation in heterogeneous mixtures of fuel droplets, fuel vapor and air," *Symposium (International) on Combustion*, vol. 18, no. 1, pp. 321–328, 1981.

[4] A. P. Wandel, N. Chakraborty, and E. Mastorakos, "Direct numerical simulations of turbulent flame expansion in fine sprays," *Proc. of the Combustion Institute*, vol. 32 II, no. 2, pp. 2283–2290, 2009.

[5] A. Neophytou, E. Mastorakos, and R. S. Cant, "The internal structure of igniting turbulent sprays as revealed by complex chemistry DNS," *Combustion and Flame*, vol. 159, no. 2, pp. 641–664, 2012.

[6] C. E. Polymeropoulos and S. Das, "The effect of droplet size on the burning velocity of kerosene-air sprays," *Combustion and Flame*, vol. 25, no. C, pp. 247–257, 1975.

[7] Y. Mizutani and T. Nishjmoto, "Turbulent Flame Velocities in Premixed Sprays Part I. Experimental Study," *Combustion Science and Technology*, vol. 6, no. 1-2, pp. 1–10, sep 1972.

[8] G. D. Myers and A. H. Lefebvre, "Flame propagation in heterogeneous mixtures of fuel drops and air," *Combustion and Flame*, vol. 66, no. 2, pp. 193–210, 1986.

[9] G. A. Richards and A. H. Lefebvre, "Turbulent flame speeds of hydrocarbon fuel droplets in air," *Combustion and Flame*, vol. 78, no. 3-4, pp. 299–307, 1989.

[10] P. M. de Oliveira, P. M. Allison, and E. Mastorakos, "Forced ignition of dispersions of liquid fuel in turbulent air flow," in *55th AIAA Aerospace Sciences Meeting*. Dallas: American Institute of Aeronautics and Astronautics, jan 2017, pp. 1–8.

[11] J. Kariuki and E. Mastorakos, "Experimental investigation of flame propagation in droplet laden mixtures," *Combustion and Flame*, vol. to appear, 2016.

[12] J. T. Edwards, "Reference Jet Fuels for Combustion Testing," in *55th AIAA Aerospace Sciences Meeting*. Dallas: American Institute of Aeronautics and Astronautics, jan 2017.

[13] A. Neophytou and E. Mastorakos, "Simulations of laminar flame propagation in droplet mists," *Combustion and Flame*, vol. 156, no. 8, pp. 1627–1640, aug 2009.